Advances in Magnetic Field Sensors

Pavel Ripka, *Member, IEEE*, and Michal Janošek

***Abstract*—The most important milestone in the field of magnetic sensors was when AMR sensors started to replace Hall sensors in many applications where the greater sensitivity of AMRs was an advantage. GMR and SDT sensors finally found applications. We also review the development of miniaturization of fluxgate sensors and refer briefly to SQUIDs, resonant sensors, GMIs, and magnetomechanical sensors.**

***Index Terms*—Magnetic field sensors, magnetic sensors, magnetometers, magnetoresistors.**

I. Introduction

In this paper, we make a review of recent advances in the technology and applications of magnetic sensors, which have appeared in the past seven years following the publication of a comprehensive book on magnetic sensors and magnetometers [1]. Here, we concentrate primarily on thin-film devices, as magnetic sensors based on bulk functional magnetic materials were recently reviewed in [2].

In recent years, anisotropic magnetoresistive (AMR) sensors with integrated flipping and feedback coils have become standard off-the-shelf devices for use in medium-accuracy applications such as compasses for mobile devices. After many years of development, giant magnetoresistive (GMR) sensors have finally found applications in angular sensing. Spin-dependent tunneling (SDT) devices are used for applications that require the smallest sensor size. Exciting improvements have been achieved in the sensitivity of resonance magnetometers, but most of the new devices are still in the laboratory phase. Despite the recent achievements in giant magnetoimpedance (GMI) sensors and orthogonal fluxgates, these devices are still far from the parameters achieved by classical longitudinal fluxgate sensors.

The development of magnetic sensor technology has been slow and gradual. Most breaking news about nanosensors with picotesla resolution has turned out to be a bubble. Exaggerated advertisements have resulted in inflated parameters for magnetic devices; we will try to show which factors are critical for real applications of magnetic sensors.

II. Flux Concentrators

Flux concentrators made of high-permeability material increase the sensitivity of any magnetic sensor. At present, they are integrated into the package of some Hall sensors and magnetoresistors. They can also be used to deflect the sensing direction so that the Hall sensor is sensitive to the in-plane field [3]. Similar concentrators are used to shield inactive sensors connected in a Wheatstone bridge in some GMR sensors.

The weak points of flux concentrators include remanence, nonlinearity, the danger of saturation, and temperature dependence. It is important to use high-permeability material and not excessively high magnetic gain, so that the temperature dependence of the gain factor is low.

An extreme case of a high-gain setup is a low-noise Hall sensor with 20-cm long concentrators having a 100 μm air gap [4]. The magnetic gain is 600, and the achieved noise level is 100 $\mathrm{pT}/\sqrt{\mathrm{Hz}}$@1 Hz. Such a sensor is a rarity, as much smaller fluxgates have lower noise. However, a similar sensor configuration was successfully used in one device in combination with an induction magnetometer to measure also the dc component [5].

Modulation of the permeability of the material by an excitation field may help to shift the signal frequency out of the $1/f$ noise range of the Hall sensor. The miniature sensor described in [6] uses permeability modulation of the 5-mm-long wire concentrator and the achieved noise level is 8 $\mathrm{nT}/\sqrt{\mathrm{Hz}}$@1 Hz. Modulation of the dc field can also be achieved by periodically moving the concentrator using an Microelectromechanical System (MEMS) [7]. However, compared to field modulation by changing the permeability (which is also used in fluxgate sensors), this approach is rather complicated. Until now, competitive results have not been achieved. It is also possible to modulate the permeability by increasing the temperature above the Curie point [8], but this is rather impractical, as the working temperature of such a device is limited.

Flux concentration can be also performed by a super-conducting loop (a flux-to-field transformer), which has been successfully used in GMR-mixed sensors [9]; the achieved gain factor was 1000. However, to achieve 100 $\mathrm{pT}\sqrt{\mathrm{Hz}}$@1 Hz the device requires 4.2 K temperature. For 77 K temperature, the noise is increased to 600 $\mathrm{pT}\sqrt{\mathrm{Hz}}$@1 Hz.

III. Hall Sensors

Most of the magnetic sensors that are produced use the Hall effect. The Hall sensitivity of silicon sensors is typically 1 mV/mT for a 1 mA current. Higher sensitivity can be achieved with thin-film InSb (typ. 5 mV/mT) or InAs (typically, 2 mV/mT). InAs exhibits lower temperature dependence of the Hall voltage compared to Si and InSb, and the working range of InAs devices is also superior: it exceeds the -40 °C to $+150$ °C range required for automotive applications. A promising Hall sensor was made using silicon-on-insulator (SOI) technology: 1 $\mu\mathrm{T}/\sqrt{\mathrm{Hz}}$@1 Hz noise was achieved for an 80-μm wide, 50-nm thick sensor [11].

Manuscript received October 02, 2009; revised December 16, 2009; accepted February 07, 2010. Current version published April 07, 2010. This is an expanded paper from the IEEE SENSORS 2008 Conference. The associate editor coordinating the review of this paper and approving it for publication was Dr. Patrick Ruther.

The authors are with the Department of Measurement, Czech Technical University, Faculty of Electrical Engineering, Technicka 2, 166 27 Praha 6, Czech Republic (e-mail: ripka@fel.cvut.cz; janosem@fel.cvut.cz).

Color versions of one or more of the figures in this paper are available online at http://ieeexplore.ieee.org.

Digital Object Identifier 10.1109/JSEN.2010.2043429

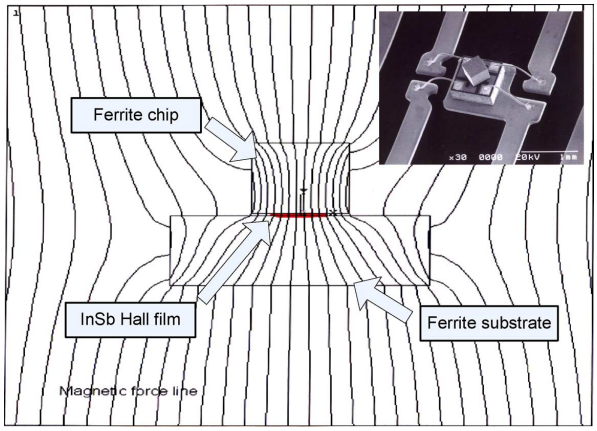

Fig. 1. Magnetic force lines of field concentrators for a thin-film Hall sensor (FEM simulation), courtesy of Asahi Kasei Electronics.

Two-dimensional quantum-well multilayer heterostructures based on GaAs are promising for low-noise Hall sensors: 100 $\mathrm{nT}/\sqrt{\mathrm{Hz}}$@1 Hz noise was achieved with external spinning-current electronics [10], which was further improved threefold by using leakage-free switches.

Fig. 1 shows an off-the-shelf InSb Hall sensor with an integrated ferrite concentrator (Asahi Kasei, BW series): the InSb thin-film Hall sensor is sandwiched between two ferrite pieces. The figure shows the flux lines simulated by FEM and a microphotograph of the device.

The integrated CMOS[1] micro-Hall plate sensor with an active area of 2.4 μm$\times$ 2.4 μm supplied by the spinning current has noise of 300 $\mathrm{nT}/\sqrt{\mathrm{Hz}}$@1 Hz [12]. CMOS technology allows to make intelligent Hall sensors with an on-chip digital signal processing part, these sensors can communicate digitally and perform sophisticated error corrections. One example is the ability to compensate not only the temperature dependence of the sensor itself, but also the temperature dependence of the magnetic circuit enclosing the sensor (temperature coefficient of the permeability, changes in the airgap, etc.)

IV. AMR Sensors

Single-domain ferromagnetic thin films exhibit AMR: their electric resistance is higher by about 2% in the direction of the magnetization than in the perpendicular direction (this effect exists in non-magnetic metals, but it is much weaker). AMR sensors are more sensitive than Hall sensors, and they exhibit better offset stability because they do not suffer from the piezo effect. The development of AMR sensors was driven by the need to replace inductive reading heads in hard disks. In this application, they were later replaced by GMR and SDT sensors, as these allowed higher storage densities due to their smaller size. Linear AMR sensors are at present produced mainly by NXP (Philips), Honeywell and Sensitec. They can have 10 nT resolution, but, unlike Hall sensors, the driving and signal processing electronics cannot be integrated on the same chip.

Almost all commercially available AMR sensors use a "barber pole" structure, in which aluminum stripes sputtered on permalloy strips deflect the direction of the current by 45° and make the characteristics linear. Four such meander-shaped elements are connected into a Wheatstone bridge.

[1]Complementary Metal-Oxide-Semiconductor.

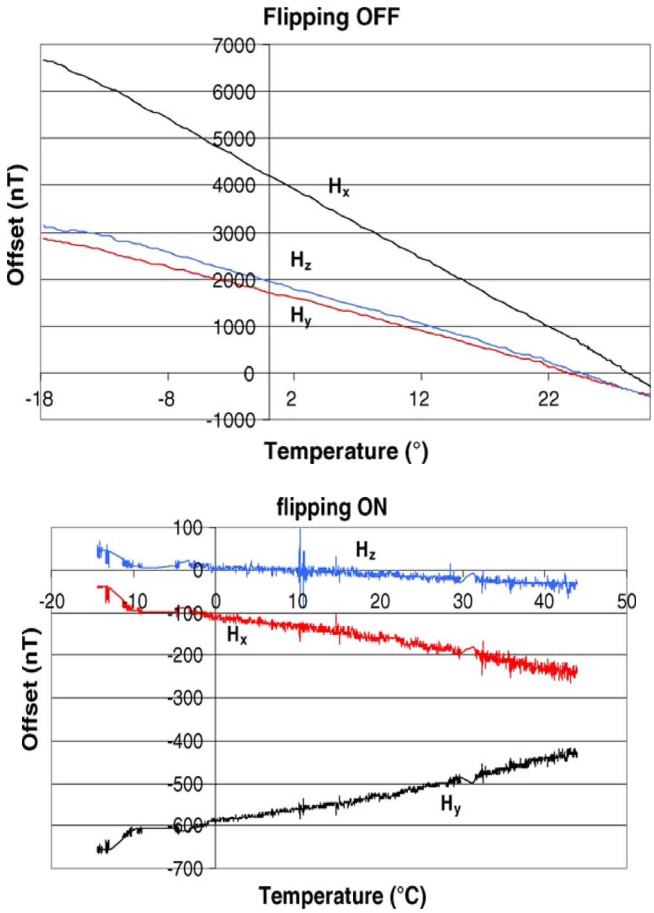

Fig. 2. (Top) Temperature offset drift of three Honeywell HMC 1001 AMR sensors without flipping, from [17]. (Bottom) Temperature offset drift of three Honeywell HMC sensors 1001 with periodical flipping, from [17].

The principles of AMR sensors are described in [13], comparative measurements of the noise of various magnetoresistors are shown in [14]. The best AMR sensors have a noise of 200 $\mathrm{pT}/\sqrt{\mathrm{Hz}}$@1 Hz [15]; however, it is difficult to achieve pT noise values with the whole AMR magnetometer; realistic resolution is 10 nT [16].

A. Flipping

The proper function of an AMR sensor is based on the single-domain state of the magnetic layer. A good technique for guaranteeing this is periodical "flipping" – remagnetization of the sensor structure by short pulses into a coil (which is usually integrated on the chip). Bipolar flipping is used for low-field sensors, because it also reduces the sensor offset and crossfield error. Fig. 2 shows the offset drift of flipped sensors in a tri-axial AMR magnetometer: without flipping, the drift was typically 100 $\mathrm{nT}/^{\circ}\mathrm{C}$.

B. Magnetic Feedback

Another technique for improving the accuracy of any magnetic sensor is feedback compensation of the measured field. Modern AMR sensors have an integrated flat feedback coil, which simplifies the magnetometer design, but may also cause new design problems, as the compensating field is much less homogeneous than that of a solenoid–this may cause linearity error. The temperature coefficient of sensitivity of a typical

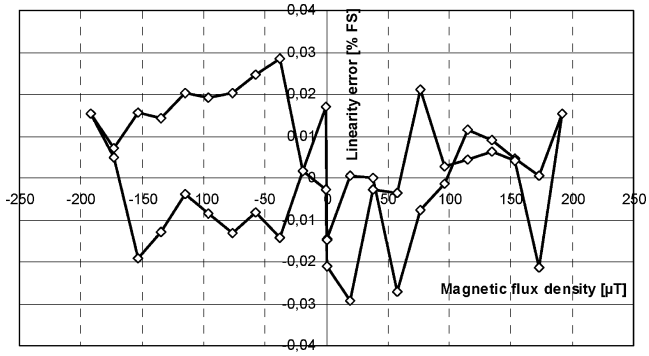

Fig. 3. Linearity error of a Philips KMZ 51 AMR sensor, feedback compensated by using an internal coil. Hysteresis is also visible from the measurement cycle [18].

AMR sensor may be reduced from 0.25%/K to 0.01%/K by using negative feedback with a sufficient gain; the remaining temperature dependence is due to the temperature coefficient of the field factor of the feedback coil. The temperature coefficient of the offset remains the same (typically 10 nT/K, but varies from piece to piece, even between sensors from the same batch), as feedback has no effect on this parameter. With feedback compensation, the linearity error may be below 300 ppm of the full-scale, as shown in Fig. 3 [18].

C. Crossfield Error

AMR sensors suffer from cross-field error: the output voltage V depends not only on the measured field H_{y}, but also on the field component H_{x}, perpendicular to the sensing direction

$$V = 2I\Delta R\frac{H_Y}{H_X + H_0}$$

where ΔR is the maximum resistance change and I is the bridge current.

From the previous equation, we can see that the cross-field error (response to H_{x}) is zero for $\mathrm{H_y} = 0$. The magnetic feedback that automatically compensates $\mathrm{H_y}$ can achieve this (Method 1). However, in some cases this is not possible due to limitations of power, circuit complexity or speed. Honeywell has released new sensors with "reduced cross-field error" by increasing the $\mathrm{H_0}$ (Method 2); but this also reduces sensitivity and thus increases sensor noise in field units.

Cross-field error may cause a 2.4-degree azimuth error for the AMR compass. This error can be compensated numerically if we know $\mathrm{H_0}$ and measure the field in two directions, or better in three directions (Method 3) [19]. If periodic flipping is used and each output is read separately, the cross-field error can be suppressed simply by averaging the outputs for the "SET" and "RESET" flipping polarities (Method 4). More complicated calculations may lead to better correction of the crossfield error (Method 5), and, in some cases, two components of the external field can even be measured using a single sensor [20]. Methods for suppressing the cross-field error are summarized in Table I.

TABLE I
METHODS FOR REDUCING THE CROSSFIELD ERROR IN AMRS

Method	Advantage	Disadvantage
Feedback compensation of the measured field $\mathrm{H_y}$	Fully analog method	Non-homogeneity of the compensation field. Power consumption
Increasing $\mathrm{H_o}$	Implemented during sensor production, no postprocessing	Decreased sensitivity, increased noise
Numerical correction using 3 sensors	Flipping not necessary, lowest power consumption	Requires complicated calibration. Digital processing necessary
Flipping and averaging	Simple, can be analog	Residual error (typically 1%)
Flipping and calculation	Small error	Digital processing required

V. GMR AND SDT SENSORS

GMR and SDT magnetoresistors are made of magnetic multilayers separated by very thin non-magnetic conducting (GMR) or insulating (SDT) layers. The electrical resistance of these structures depends on the direction of their magnetization. In general, if the magnetic layers are magnetized in the same direction, the resistance is smaller than for layers magnetized in opposite (antiparallel) directions. The external measured field usually controls the magnetization direction in the "free" layer, while the other "pinned" layer has fixed magnetization.

In order to compensate the basic temperature sensitivity, these devices are made as Wheatstone bridges. A bipolar response of the GMR bridge branches can be achieved by a DC bias field or, in the case of a spin valve, by changing the orientation of the magnetization of the magnetically hard pinning layer [21].

The most promising industrial application of GMR sensors is in angular sensing. The magnetization direction of the free layer of the spin-valve is rotated by the permanent magnet. If the free layer is saturated, the sensor output does not depend on the magnet distance, only on the measured angle.

Recently developed GMR sensors have increased their temperature stability: Hitachi has reported only a 20% sensitivity change between -40 °C to $+120$ °C, and 30 minutes of survival at 250 °C. However, large magnetic fields—especially at elevated temperatures—can destroy GMR spin valves due to changes in the magnetization of the pinning layer. This danger does not exist for Hall sensors and AMR magnetoresistors.

In the case of SDT sensors, high coercivity and low linearity remain a serious problem [22]; however, a digital magnetometer with a SDT sensor reported in [23] exhibited 1 $\mu\mathrm{T}$ resolution and a linear range of ± 1 mT.

GMR and SDT sensors have $1/\mathrm{f}$ noise with cutoff frequency in the order of MHz, and the reported noise levels are quite high [24]. Picotesla-detection predictions are usually based only on thermal noise, and they did not take magnetic $1/\mathrm{f}$ noise into account [25]. Fig. 4 shows that magnetoresistors in general have much higher noise than fluxgate sensors. However, their main advantage, especially in the case of SDT sensors, is their small

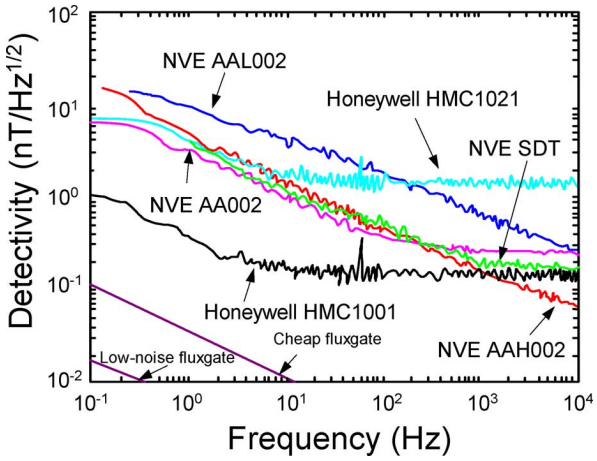

Fig. 4. Noise spectrum of magnetoresistors and fluxgate sensors. HMC 1001 and 1021 are AMR magnetoresistors, NVE AAxx are GMR magnetoresistors, and NVE SDT is a prototype of a spin-dependent tunelling device. The data for a "cheap fluxgate" represent typical noise of Applied Physics Model 533 and similar devices. The data for "low-noise fluxgate" is taken from [27]. Adopted from [14].

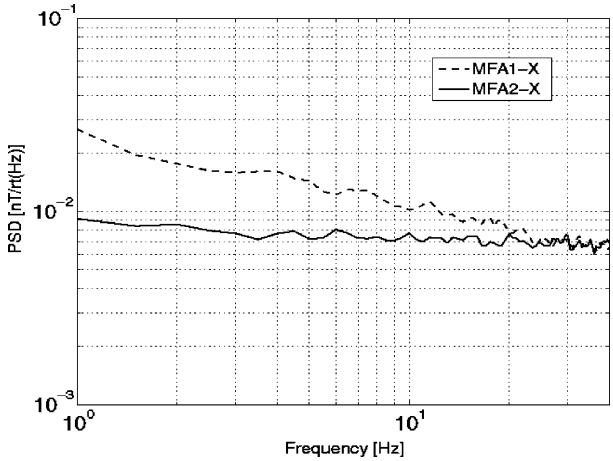

Fig. 5. Noise of a fully digital fluxgate magnetometer with CMOS ASIC electronics – without (top trace) and with dynamic offset cancellation (bottom trace)– from [33].

size and thus high spatial resolution. This is critical when measuring small objects such as magnetic microbeads for medical applications [26], and also where a small distance from the magnetic source is required.

VI. Fluxgate Sensors

Fluxgate sensors measure DC and low-frequency AC fields up to approximately 1 mT with a resolution of 100 pT and with linearity-error less than 10 ppm. Their operation is based on modulation of the permeability of the soft magnetic core, which creates changes in the dc flux ("flux-gating") of the pickup coil wound around the sensor core. The output voltage is on the second harmonics of the excitation frequency, as permeability reaches its minimum and maximum twice in each excitation cycle.

Most fluxgates have a ring core and the same direction of the excitation and measured fields [27]. The Vacquier-type fluxgate, which has two straight cores and solenoidal windings, was studied in [28]. Another form of core material is magnetic wire. Despite the higher noise, the Vacquier-type fluxgate has the following important advantages: 1) due to very low demagnetization, the sensor is insensitive to perpendicular fields and 2) unlike ring-core sensors, the sensing direction is well defined by the direction of the core. This is utilized in gradiometers, which require very high directional stability.

In order to achieve low remanence (or a small perming effect, which is an offset change after the sensor is subjected to a magnetic shock), the excitation should very deeply saturate the core of the sensor. In order to achieve this with reasonable power consumption, nonlinear excitation tuning is often used. The resonance tank consists of the excitation coil and the parallel capacitor. In resonance, the coil current has very high peaks (typically, 1 to 4 A): once the core is saturated, the impedance of the excitation coil drops and the capacitor is discharged through this coil. Despite the high peaks, the rms value of the current is small (typically, 10 to 50 mA).

The standard method for fluxgate signal processing is phase-sensitive detection of the second harmonic component of the output voltage. Precise magnetometers developed at the Danish Technical University utilize (short-circuited) current output [29].

The best fluxgate magnetometers use a so-called Compact Spherical Coil (CSC) with three orthogonal windings for the feedback. In order to achieve a homogeneous field, the coil is wound on the surface of a sphere, as the ideal spherical coil has a homogeneous field throughout the volume inside. The external magnetic field is completely compensated, so that the three orthogonally mounted fluxgate sensors inside the coil system are in a magnetic vacuum and thus do not suffer from cross-field errors. The disadvantages of CSC are as follows:

- — large volume: in order to reduce the size of the CSC the fluxgate sensors are mounted in close vicinity and influence each other;
- — high price: complex mechanics;
- — the sensors cannot be removed without breaking the coils.

The best reported offset stability in the -18 °C to $+63$ °C range is ± 0.6 nT [30]. Nishio *et al.* investigated sensitivity, offset and noise in a wide-temperature range [31]: with a ceramic core bobbin, the offset variations were below ± 3 nT in the -180 °C to $+220$ °C range.

Digital fluxgate magnetometers [32] use two basic approaches, which can be combined:

- — replacing the analog synchronous detector by digital signal processing;
- — replacing the analog feedback loop by a delta-sigma or some other digital feedback scheme.

Digital magnetometers still do not achieve the parameters of the top analog magnetometers [33], but they are very flexible and allow for the future integration of electronics into a single ASIC chip. Using dynamic offset compensation of the input stage, the noise was lowered to 9 $\mathrm{pT}/\sqrt{\mathrm{Hz}}$@1 Hz (Fig. 5), which is sufficient for most applications in the presence of the Earth's field [34].

A. Miniature Fluxgates

As common fluxgate sensors can be quite large (diameter in units of cm for low-noise, ring-core devices), many miniaturiza-

tion approaches have been tried. Three basic types of miniature fluxgate are: 1) CMOS-based devices with flat coils; 2) sensors with microfabricated solenoids; and 3) PCB-based devices with solenoids made by tracks and vias.

CMOS microfluxgates are based on a strip of soft magnetic material on top of a flat coil system made with a metallic layer of a standard CMOS process. These flat coils serve both to excite the strip core, which is either a sputtered or an electrodeposited permalloy or a shaped amorphous material. These devices may have low-power sensor electronics integrated on the same chip. A 4×4 mm, 2-axial sensor for a wristwatch compass was reported to achieve 15 $\mathrm{nT}/\sqrt{\mathrm{Hz}}$@1 Hz noise with 92 V/T sensitivity and 10 mW power consumption [35]. A similar design using a sputtered, 1-μm-thick Vitrovac ($\mathrm{H_c} = 100\ \mathrm{A/m}$), achieved 7.4 $\mathrm{nT}/\sqrt{\mathrm{Hz}}$@1 Hz. With increased power consumption, the sensitivity was 450 V/T and the linearity was 1.15% in the ± 50-$\mu\mathrm{T}$ range [36].

A flat coil of CMOS fluxgates has, in principle, high resistance and poor magnetic coupling with the core. The efficiency of the flat coil is therefore much worse than that of a solenoid. The UV-LIGA[2] process enables the production of MEMS single-layer solenoids with 25 turns/mm [37]. A microfluxgate made using such a technology is reported in [38]. The sensor with a 30-μm electroplated permalloy core has 56 excitation turns with a total resistance of 2 Ω and 11 sensing turns. A sensitivity of 650 V/T was achieved for a 5.5-mm-long sensor with 14 mW power consumption. The noise is 32 $\mathrm{nT}/\sqrt{\mathrm{Hz}}$@1 Hz, and the practical resolution is 1 μT, which is still worse than the resolution of the best AMR sensors. To reduce the size of the sensor, the authors used the "localized core saturation" method, which led to large perming because only a part of the sensor core was saturated: 30 μT perming was observed for a 200 mT shock.

PCB-based fluxgates achieved low noise (24 $\mathrm{pT}/\sqrt{\mathrm{Hz}}$ @1 Hz) and good temperature stability (20 nT in the -20 °C to $+70$ °C range), but the minimum size achievable with this technology is about 10 mm [39].

As miniature fluxgates may have only a limited number of turns of the pickup coil, the sensitivity is lower than that of a traditional wire-wound fluxgate. This is often compensated by a higher excitation frequency (typically, 300 kHz compared to 20 kHz). Proper fluxgate excitation should deeply saturate the sensor core in order to reduce "perming" (offset the change after the sensor is exposed to a large field). The low number of turns of the excitation coil of the integrated fluxgate necessitates the use of large excitation current peaks. As the cross-sectional area of the magnetic core is small, the quality factor of the excitation coil is low in comparison with large-size fluxgates. Nonlinear excitation tuning is therefore no longer possible. One way to reduce the power consumption in the excitation circuit is to use short excitation current pulses instead of a sinewave or squarewave [40].

B. Orthogonal Fluxgates

The main advantage of an orthogonal fluxgate is that it needs no excitation coil – the sensor is excited directly by the current flowing through the core. As is usual for fluxgate sensors, the output is at the second harmonic of the excitation frequency. The orthogonal fluxgate effect in ferromagnetic wire was known since the 1950s. Some authors have observed this effect during magnetoimpedance studies, and they use the term "nonlinear magnetoimpedance" for the same effect. This effect has been studied at high frequencies in tapes [41] and in wires [42], [43]; the observed output variable was calculated as the "MI ratio," which does not keep phase information and thus does not allow the field polarity to be recognized. The use of phase-sensitive detection of the output voltage (which is a standard technique for a fluxgate) gives a clear advantage for the performance of the sensor. The disadvantage of an orthogonal fluxgate is that the necessary excitation current is usually high (typically, 20 to 100 mA). As the magnetic field in the inner part of the conductor is low, which causes perming, a favorable design is a nonmagnetic conductor covered by a magnetically soft thick layer.

A miniature orthogonal fluxgate with a planar structure, formed by a Permalloy layer electrodeposited on a rectangular copper conductor, is reported in [44]. The sensor core is only 1 mm in length, and the sensor has two flat 60-turn pickup coils. The overall dimension of the sensor chip is 1.8×0.8 mm, the sensitivity is 0.5 $\mathrm{mV}/\mu\mathrm{T}$ in a ± 200 μT linear operating range. The noise was 95 $\mathrm{nT}/\sqrt{\mathrm{Hz}}$@1 Hz with 8 mW net excitation power consumption.

The "fundamental mode" orthogonal fluxgate uses DC biased excitation; the output is on the same frequency as the excitation. As this sensor is saturated only in one polarity, the basic offset stability is poor and it can be improved by periodic switching of the excitation bias. The authors in [45] achieved a sensitivity of 1.8 $\mathrm{mV}/\mu\mathrm{T}$, offset stability of 1.2 nT/hour and a noise level of about 100 $\mathrm{pT}/\sqrt{\mathrm{Hz}}$@1 Hz with periodic bias switching (20 pT without it). In [46], the temperature coefficient of sensitivity was reduced from 6500 to 100 ppm/K using feedback compensation. A triaxial device was reported in [47], having three 38-mm-long U-shaped legs made of a single amorphous wire (125 μm diameter). The sensor achieved a noise level of 360 $\mathrm{pT}/\sqrt{\mathrm{Hz}}$@1 Hz with 4 mA excitation and 20 mA DC bias current. Another fundamental-mode fluxgate with an unusual, 5-cm-long, amorphous tubular core was presented in [48]. The orthogonal excitation field was created by a toroidal coil, which reduced the necessary excitation current to 6 mA. For a 60-mA DC-bias current, the noise achieved was 10 $\mathrm{pT}/\sqrt{\mathrm{Hz}}$@1 Hz. However, this configuration is no longer mechanically simple, which is the main advantage of the classical orthogonal configuration.

The so called "coil-less fluxgate" has no pickup coil: the sensor output is the second harmonic voltage induced between the wire terminals. The operation is based on helical anisotropy, which creates an off-diagonal component of the permeability tensor: the field in the axial direction creates axial flux and thus the longitudinal component of the induced voltage. The sensitivity achieved for a 38-mm-long sensor is 0.2 $\mathrm{mV}/\mu\mathrm{T}$ [49].

VII. Other Devices

In this short review paper, we will mention SQUID [3] magnetometers only briefly. DC SQUIDS are less noisy than the RF SQUIDS. These devices are based on a superconducting

[2]UltraViolet Lithographie, Galvanoformung, Abformung.

[3]Superconducting Quantum Interference Devices.

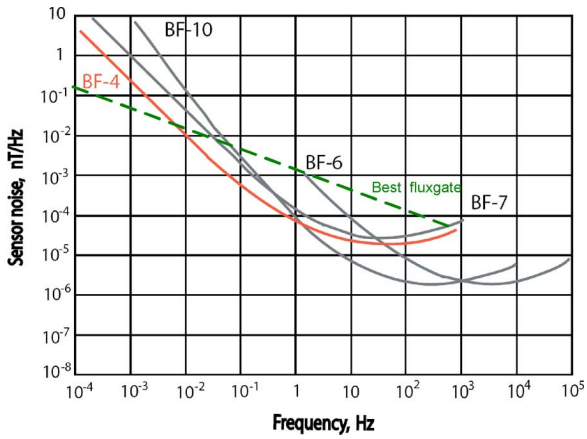

Fig. 6. Noise of popular EMI induction sensors and a low-noise fluxgate – adapted from a Schlumberger datasheet [54].

ring with two Josephson junctions [1]. In order to increase the sensitivity, a flux transformer is often used. SQUID in fact measures only field changes, not the absolute field. The noise level of a low-Tc SQUID with a flux-transformer can be as low as 1 $\mathrm{fT}/\sqrt{\mathrm{Hz}}$ and a high-Tc system can have white noise of 36 $\mathrm{fT}/\sqrt{\mathrm{Hz}}$, as shown in the excellent review by Robbes [50].

Resonant magnetometers (proton magnetometers, Overhauser magnetometers and optically pumped magnetometers) are usually very stable scalar devices which measure the absolute field value regardless of the field direction [1]. While optical magnetometers are based on Zeeman splitting, classical proton magnetometers measure the precession frequency of a proton or electron. It is known that any scalar magnetometer can be made vectorial by adding a rotating bias field and demodulating the output, but this technique degrades the sensor performance both in bandwidth and in noise. The 1 $\mathrm{fT}/\sqrt{\mathrm{Hz}}$@10 Hz noise of the spin-exchange relaxation-free (SERF) magnetometer is noticeable: the main idea of this magnetometer is to reduce spin-exchange broadening of the Zeeman resonance. SERF may reach SQUID-level performance without cryogenic cooling. This magnetometer is a vectorial one: to obtain the remaining two vectors, the field has to be again modulated. The SERF magnetometer operates only in a near-zero field, and the vapor cell must be heated. Magnetic fields higher than about 10 nT should be vectorially compensated. A recent review of these "optical atomic magnetometers," which are still experimental devices, has been presented by Budker *et al.* [51].

Induction magnetometers are based on the Faraday induction law; thus they measure the flux derivative. Instead of measuring open-circuited induced voltage, some induction magnetometers evaluate the short-circuited coil current, which in ideal conditions is proportional to the flux [1]. Induction magnetometers naturally cannot measure dc fields, but at frequencies higher than 0.01 Hz they may have lower noise than a fluxgate, if sensor dimension and mass is not an issue. Fig. 6 shows the noise spectra of several commercially available induction coils manufactured by EMI (a division of Schlumberger) [52], compared to a typical low-noise fluxgate. The length of the BF-4 sensor, which has the smallest noise at low frequencies, is 142 cm, and its mass is 8 kg. BF-6 and BF-10 are similar in size, but these coils are optimized for higher frequencies; the 104 cm long BF-7 sensor weighs only 2 kg. A small induction sensor was described in [53], it is 10 cm in length and weighs only 11 g; its noise is 2 $\mathrm{pT}/\sqrt{\mathrm{Hz}}$@1 Hz. In [54], the authors constructed a 3-axial satellite induction magnetometer using similar sensors with 17-cm-long cores, and the overall mass weight of the 3-axial probe, including the holder device, was only 600 g. The frequency range was 0.1 Hz to 10 kHz, keeping the noise level of 2 $\mathrm{pT}/\sqrt{\mathrm{Hz}}$@1 Hz. A detailed review of induction magnetometers appeared recently in [55].

The GMI effect is based on the field-dependent change of the penetration depth [56]. The effect has only limited practical applications, as it is temperature dependent, gives low sensitivity and the characteristics are nonlinear and unipolar. The temperature dependence of the GMI effect is analyzed in [57]–[59]. GMI sensors are used in compass modules for some mobile phones [59], but the achievable accuracy is not clearly specified. The lowest achieved noise level extrapolated to 1 Hz (using $1/\mathrm{f}$ noise rule) is 100 $\mathrm{pT}/\sqrt{\mathrm{Hz}}$@1 Hz for a 10-mm-long device presented in [60]. Due to the small diameter of the wire core, these sensors may have high spatial resolution and thus serve for detecting microbeads [61]. The disadvantage of GMI and similar sensors compared to a fluxgate is the perming effect, because the ferromagnetic core is usually not demagnetized during sensor operation.

A synthetic **magneto-electric sensor** with 130 V/T sensitivity was presented in [62]. It contains a sandwich made from magnetostrictive and piezoelectric materials. The measured field causes strain in the magnetostrictive layer. This strain is coupled to the piezoelectric layer, where the output voltage is generated. The achieved sensitivity for a 10-cm-long Metglas-PZT fiber laminate was 3000 V/T [63].

Other sensors are based on changing the **resonance frequency** of free-standing elements manufactured by MEMS technology. The preliminary results on large-scale models of a "xylophone magnetometer" were promising, but until now low noise has not been achieved on a small scale using MEMS polysilicon technology [64].

The micromachined **Lorentz force magnetic sensor** achieved field resolution of 10 $\mathrm{nT}/\sqrt{\mathrm{Hz}}$ for a 100 μA measuring current [65]. The Lorentz force, which is proportional to the measured field and the measuring current, deflects the free-standing MEMS structure. The motion is made periodic by applying an AC measuring current, usually at mechanical resonance frequency. The advantage of Lorentz force magnetometers is their high linearity and the possibility to change their range widely by selecting the measuring current. The sensor can work up to 50 T [66]. A detailed discussion on these sensors can be found in [67].

Magnetic sensors used for measuring electric **current, position, and mechanical torque** are described in [68], and therefore do not appear in this review. The most important achievements in these devices are the AMR gradient bridge for current sensors and polarized-band torque sensors for automotive applications. Sensors for magnetic **nondestructive testing** have been reviewed in [69].

TABLE II
PROPERTIES OF COMMON MAGNETIC FIELD SENSORS

	Hall with field concentrators (Sentron CSA-1VG)	AMR (Philips KMZ 51, Honeywell, HMC1001)	AMR flipped+feedback (KMZ 51 [18])	Fluxgate Billingsley TFM100
linear range	5 mT	300 μT	300 μT	100 μT
size	6 mm	6 mm	6 mm	15 mm
linearity	0.1 < 0.2 %	1 %	40 ppm	20 ppm
sensitivity TC	200 ppm/K	600 ppm/K	20 ppm/K	20 ppm/K
offset @ 25°C	50 μT	< 10 μT	< 1 μT	10 nT
offset TC	600 nT/K	100 nT/K	2 nT/K	0.2 nT/K
$noise_{RMS}$ (0.1-10 Hz)	1 μT	10 nT(1 nT)	10 nT	<100 pT
perming, hysteresis	1 μT	300 nT	10 nT	< 1 nT
BW	100 kHz	100 kHz	100 Hz	3.5 kHz
power consumption	55 mW	30 mW	100mW	350 mW

VIII. CONCLUSION

We have briefly referred to the main recent advances in magnetic field sensors. So far, there is always a tradeoff between the size of a sensor and its parameters. The progress of miniaturization is not likely to be skipped by novel nanosized sensors without using new physical principles. In many applications, such as detection of magnetic microbeads, micromagnetic scanning or NDT, sensor size is an issue and is often the only selection criterion, either because of the need for spatial resolution or because of the weak point-like sources. However, in cases where a large detection distance cannot be avoided, parameters such as noise (detectivity) become more important. In more demanding applications, such as precise compasses, positioning and tracking devices, the linearity, temperature coefficients and even cross-field sensitivity of the sensor also start to be more important than noise, which is often the only parameter that is mentioned .

Table II compares important parameters of the most popular solid-state magnetic field sensors. We give values for some of the best commercially-available sensors in each class.

REFERENCES

[1] *Magnetic Sensors and Magnetometers*, P. Ripka, Ed.. New York: Artech, 2001.

[2] P. Ripka, "Sensors based on bulk soft magnetic materials: Advances and challenges," *JMMM*, vol. 320, pp. 2466–2473, 2008.

[3] R. S. Popovic, *Hall Effect Devices*. London, U.K.: Institute of Physics, 2004.

[4] P. Leroy, C. Coillot, V. Mosser, A. Roux, and G. Chanteur, "Use of magnetic concentrators to highly improve the sensitivity of Hall effect sensors," *Sensor Lett.*, vol. 5, pp. 162–166, 2007.

[5] P. Leroy *et al.*, "An ac/dc magnetometer for space missions: Improvement of a Hall sensor by the magnetic flux concentration of the magnetic core of a searchcoil," *Sens. Act. A*, vol. 142, pp. 503–510, 2008.

[6] A. Quasimi, C. Dolabdjian, D. Bloyet, and V. Mosser, "Improvement of the mu-hall magnetic sensor sensitivity at low frequency," *IEEE Sensors J.*, vol. 4, pp. 160–166, 2004.

[7] O. Arif, E. R. Nowak, A. S. Edelstein, G. A. Fischer, C. A. Nordman, and S. F. Cheng, "Magnetic-field dependence of the noise in a magnetoresistive sensor having MEMS flux concentrators," *IEEE Trans. Magn.*, vol. 42, pp. 3306–3308, 2006.

[8] W. Wang and J. Zhenye, "Thermally modulated flux concentrator for minimizing $1/f$ noise in magnetoresistance-based field sensors," *IEEE Trans. Magn.*, vol. 44, pp. 4003–4006, 2008.

[9] M. Pannetier-Lecoeur *et al.*, "RF response of superconducting-GMR mixed sensors, application to NQR," *IEEE Trans. Appl. Superc.*, vol. 2, pp. 598–601, 2007.

[10] A. Kerlain and V. Mosser, "Low frequency noise suppression in III-V Hall magnetic microsystems with integrated switches," *Sensors Lett.*, vol. 5, pp. 192–195, 2007.

[11] Y. Haddab, V. Mosser, M. Lysowec, J. Suski, L. Demeus, C. Renaux, S. Adriensen, and D. Flandre, "Low-noise SOI Hall devices," *Proc. SPIE.*, vol. SPIE-5115, pp. 196–203, May 2003.

[12] P. Kejik *et al.*, "An integrated micro-Hall probe for scanning magnetic microscopy," *Sens. Act. A*, vol. 129, pp. 212–215, 2006.

[13] S. Tumanski, *Thin Flm Magnetoresistive Sensors*. Bristol, U.K.: IOP Publishing, 2001.

[14] N. A. Stutzke *et al.*, "Low-frequency noise measurements on commercial magnetoresistive magnetic field sensors," *J. Appl. Phys.*, vol. 7, no. 10: Art. 10Q107, 2005.

[15] E. Zimmermann, A. Verweerd, W. Glaas, A. Tillmann, and A. Kemna, "An AMR sensor-based measurement system for magnetoelectrical resistivity tomography," *IEEE Sensors J.*, vol. 5, pp. .233–241, 2005.

[16] A. Bertoldi *et al.*, "Magnetoresistive magnetometer with improved bandwidth and response characteristics," *Rev. Sci. Instrum.*, vol. 76, pp. 065106-1–065106-6, 2005.

[17] J. Včelák, P. Ripka, A. Platil, J. Kubík, and P. Kašpar, "Errors of AMR compass and methods of their compensation," *Sens. Actuators A*, vol. 129, pp. 53–57, 2006.

[18] M. Vopálenský, P. Ripka, and A. Platil, "Precise magnetic sensors," *Sens. Actuators A*, vol. 106, pp. 38–42, 2003.

[19] J. Kubik, J. Vcelak, and P. Ripka, "On cross-axis effect of the anisotropic magnetoresistive sensors," *Sens. Actuators A*, vol. 129, pp. 15–19, 2006.

[20] P. Ripka, M. Janošek, and M. Butta, "Using the crossfield error in AMR," in *Intermag 2009 Digests*, 2009, pp. 129–130.

[21] M. Pannetier-Llecoeur, C. Fermon, A. Devismes, E. Kerr, and L. Vieuxrochaz, "Low noise magnetoresistive sensors for current measurement and compasses," *J. MMM*, vol. 316, pp. e246–e248, 2007.

[22] A. Jander, C. A. Nordman, A. V. Pohm, and J. M. Anderson, "Chopping techniques for low-frequency nanotesla spin-dependent tunneling field sensors," *J. Appl. Phys.*, vol. 93, pp. 8382–8384, 2003.

[23] J. Deak, A. Jander, E. Lange, S. Mundon, D. Brownell, and L. Tran, "Delta-sigma digital magnetometer utilizing bistable spin-dependent-tunneling magnetic sensors," *J. Appl. Phys.*, vol. 99, pp. 08B320–08B320-3, 2006.

[24] R. Ferreira, P. Wisniowski, P. P. Freitas, J. Langer, B. Ocker, and W. Maass, "Tuning of MgO barrier magnetic tunnel junction bias current for picotesla magnetic field detection," *J. Appl. Phys.*, vol. 99, pp. 08K706–08K706-3, 2006.

[25] P. P. Freitas, R. Ferreira, S. Cardoso, and F. Cardoso, "Magnetoresistive sensors," *J. Phys. Condens. Matter*, vol. 19, p. 165221, 2007.
[26] L. Xu, H. Yu, S.-J. Han, S. Osterfeld, R. L. White, N. Pourmand, and S. X. Wang, "Giant magnetoresistive sensors for DNA microarray," *IEEE Trans. Magn.*, vol. 44, pp. 3989–3991, 2008.
[27] P. Ripka, "Advances in fluxgate sensors," *Sens. Actuators A*, vol. 106, pp. 8–14, 2003.
[28] C. Moldovanu, P. Brauer, O. V. Nielsen, and J. R. Petersen, "The noise of the Vacquier type sensors referred to changes of the sensor geometrical dimensions," *Sens. Act. A: Phys.*, vol. 81, no. 1–3, pp. 197–199, 2000.
[29] F. Primdahl, J. M. G. Merayo, and P. Brauer, "Fluxgate magnetometry for precise mapping of the Earth's field," *Sensors Lett.*, vol. 5, pp. 110–112, 2007.
[30] F. Primdahl, T. Risbo, J. M. G. Merayo, P. Brauer, and L. Tøffner-Clausen, "In-flight spacecraft magnetic field monitoring using scalar/vector gradiometry," *Meas. Sci. Technol.*, vol. 17, no. 6, pp. 1563–1569, 2006.
[31] Y. Nishio, F. Tohyama, and N. Onishi, "The sensor temperature characteristics of a fluxgate magnetometer by a wide-range temperature test for a Mercury exploration satellite," *Meas. Sci. Technol.*, vol. 18, pp. 2721–2730, 2007.
[32] A. Cerman, A. Kuna, P. Ripka, and J. M. G. Merayo, "Digitalization of highly precise fluxgate magnetometers," *Sens. Actuators A*, vol. 121/2, pp. 421–429, 2005.
[33] W. Magnes *et al.*, "A sigma-delta fluxgate magnetometer for space applications," *Meas. Sci. Technol.*, vol. 14, pp. 1003–1012, 2003.
[34] W. Magnes *et al.*, "Highly integrated front-end electronics for spaceborne fluxgate sensors," *Meas. Sci. Technol.*, vol. 19, no. Article 115801, 2008.
[35] P. M. Drljaca, P. Kejik, F. Vincent, D. Piguet, and R. S. Popovic, "Low-power 2-D fully integrated CMOS fluxgate magnetometer," *IEEE Sensors J.*, vol. 5, pp. 909–915, 2005.
[36] A. Baschirotto *et al.*, "A fluxgate magnetic sensor: From PCB to micro-integrated technology," *IEEE Trans. Instrum. Meas*, vol. 56, pp. 25–31, 2007.
[37] M. Woytasik, J.-P. Grandchamp, E. Dufour-Gergam, J.-P. Gilles, S. Megherbi, E. Martincic, H. Mathias, and P. Crozat, "Two- and three-dimensional microcoil fabrication process for three-axis magnetic sensors on flexible substrates," *Sens. Act. A: Phys.*, vol. 132, pp. 2–7, 2006.
[38] P.-M. Wu and C. H. Ahn, "Design of a low-power micromachined fluxgate sensor using localized core saturation method," *IEEE Sensors J.*, vol. 8, pp. 308–313, 2008.
[39] J. Kubík, L. Pavel, and P. Ripka, "PCB racetrack fluxgate sensor with improved temperature stability," *Sens. Act. A Phys.*, vol. 130, pp. 184–188, 2006.
[40] J. Kubik, L. Pavel, P. Ripka, and P. Kaspar, "Low-power printed circuit board fluxgate sensor," *IEEE Sensors J.*, vol. 7, pp. 179–183, 2007.
[41] A. Garcia-Arribas *et al.*, "Non-linear magnetoimpedance in amorphous ribbons: Large asymmetries and angular dependence," *Sens. Act. A, Phys.*, vol. 129, pp. 275–278, 2006.
[42] G. V. Kurlyandskaya, A. Garcia-Arribas, and J. M. Barandiaran, "Advantages of nonlinear giant magnetoimpedance for sensor applications," *Sens. Act. A*, vol. 106, pp. 234–239, 2003.
[43] J. G. S. Duque *et al.*, "The effect of helical magnetoelastic anisotropy on magnetoimpedance and its second harmonic component in amorphous wires," *JMMM*, vol. 271, pp. 390–395, 2004.
[44] O. Zorlu, P. Kejik, and R. S. Popovic, "An orthogonal fluxgate-type magnetic microsensor with electroplated Permalloy core," *Sens. Act. A, Phys.*, vol. 135, pp. 43–49, 2007.
[45] K. Goleman and I. Sasada, "High sensitive orthogonal fluxgate magnetometer using a Metglas ribbon," *IEEE Trans. Magn.*, vol. 42, pp. 3276–8, 2006.
[46] A. Plotkin, E. Paperno, A. Samohin, and I. Sasada, "Compensation of the thermal drift in the sensitivity of fundamental-mode orthogonal fluxgates," *J. Appl. Phys.*, vol. 99, pp. 08B305–08B305-3, 2006.
[47] K. Goleman and I. Sasada, "A triaxial orthogonal fluxgate magnetometer made of a single magnetic wire with three U-shaped branches," *IEEE Trans. Magn.*, vol. 43, pp. 2379–2381, 2007.
[48] E. Paperno, E. Weiss, and A. Plotkin, "A tube-core orthogonal fluxgate operated in fundamental mode," *IEEE Trans. Magn.*, vol. 44, pp. 4018–4031, 2008.
[49] M. Butta, P. Ripka, S. Atalay, F. E. Atalay, and X. P. Li, "Fluxgate effect in twisted magnetic wire," *JMMM*, vol. 320, pp. e974–e978, 2008.
[50] D. Robbes, "Highly sensitive magnetometers—A review," *Sens. Act. A, Phys.*, vol. 129, pp. 86–93, 2006.
[51] D. Budker and M. V. Romalis, "Optical magnetometry," *Nature Phys.*, vol. 3, pp. 227–234, 2007.
[52] BF EM4 Datasheet, Schlumberger: EMI Technology Center. [Online]. Available: http://www.slb.com/content/about/technology/emi_bf_sensor.asp
[53] C. Coillot, J. Moutoussamy, P. Leroy, G. Chanteur, and A. Roux, "Improvements on the design of search coil magnetometer for space experiments," *Sensor Lett.*, vol. 5, pp. 167–170, 2007.
[54] A. Roux *et al.*, "The search coil magnetometer for THEMIS," *Space Sci. Rev.*, vol. 141, pp. 265–275, 2008.
[55] S. Tumanski, "Induction coil sensors," *Measure. Sci Technol.*, vol. 18, pp. R31–R46, 2007.
[56] K. Knobel, M. Vázquez, and L. Kraus, "Giant Magnetoimpedance," in *Handbook of Magnetic Materials*, K. H. J. Buschow, Ed. New York: Elsevier, 2003, vol. 15, pp. 497–563.
[57] M. Michal, R. Pavel, and K. Ludek, "Temperature offset drift of GMI sensors," *Sens. Act. A*, vol. 147, pp. 415–418, 2008.
[58] B. Hernando, J. Olivera, M. L. Sanchez, V. M. Prida, and R. Varga, "Temperature dependence of magnetoimpedance and anisotropy in nanocrystalline finemet wire," *IEEE Trans. Magn.*, vol. 44, pp. 3965–3968, 2008.
[59] Y. Nakamura, T. Uchiyama, C. M. Cai, and K. Mohri, "PWM-type amorphous wire CMOS IC magneto-impedance sensor having high-temperature stability," *IEEE Trans. Magn.*, vol. 44, pp. 3981–3984, 2008.
[60] D. Robbes, C. Dolabdjian, and Y. Monfort, "Performances and place of magnetometers based on amorphous wires compared to conventional magnetometers," *J. Mag. Mag. Mat.*, vol. 249, pp. 393–397, 2002.
[61] D. Kim, H. Kim, S. Park, W. Lee, and W. Y. Jeung, "Operating field optimization of giant magneto impedance (GMI) devices in micro scale for magnetic bead detection," *IEEE Trans. Magn.*, vol. 44, pp. 3985–3988, 2008.
[62] N. H. Duc and D. T. Huong, "Magnetic sensors based on piezoelectric–magnetostrictive composites," *J. Alloys and Compounds*, vol. 449, pp. 214–218, 2008.
[63] J. Zhai, S. Dong, Z. Xing, and J. Li, "Viehland: Geomagnetic sensor based on giant magnetoelectric effect," *Appl. Phys. Lett.*, vol. 91, p. 123513, 2007.
[64] D. K. Wickenden *et al.*, "Micromachined polysilicon resonating xylophone bar Magnetometer," *Acta Astronautica.*, vol. 52, pp. 421–425, 2003.
[65] J. Kyynäräinen *et al.*, "3D micromechanical compass," *Sensor Lett.*, vol. 5, pp. 126–129, 2007.
[66] F. Keplinger, S. Kvasnica, A. Jachimowicz, F. Kohl, J. Steurer, and H. Hauser, "Lorentz force based magnetic field sensor with optical readout," *Sens. Act. A: Phys.*, vol. 110, no. 1–3, pp. 112–118, 2004.
[67] A. L. Herrera-May *et al.*, "A resonant magnetic field microsensor with high quality factor at atmospheric pressure," *J. Micromech. Microeng.*, vol. 19, no. Art.Nr. 015016, 2009.
[68] P. Ripka and K. Závěta, "Magnetic sensors," in *Handbook of Magnetic Materials*, J. Buschow, Ed. New York: Elsevier, 2010, to be published.
[69] G. Vertesy and A. Gasparics, "Nondestructive material evaluation by novel electromagnetic methods," *Mater. Sci. Forum*, vol. 414–4, pp. 343–352, 2003.

Pavel Ripka (M'00) received the Engineering degree in 1984, the C.Sc. (equivalent to Ph.D.) in 1989, Docent degree in 1996 and in 2002 Professor degree at the Czech Technical University, Prague, Czech Republic.

During 1991–1993, he was a Visiting Researcher at the Danish Technical University and during 2001 he was Marie Curie Fellow at the National University of Ireland, Galway. From 2005 to 2006, he was a Visiting Researcher at the Institute for the Protection and the Security of the Citizen, Ispra, Italy. Currently, he is Head of the Department of Measurement, Faculty of Electrical Engineering, Czech Technical University, Prague. He is lecturing in measurements, engineering magnetism and sensors. He is a author and coauthor of 6 books, >80 journal papers and 5 patents. His main research interests are magnetic sensors, especially fluxgate and MR, eddy current detectors and their applications.

Prof. Ripka is a member the Elektra Society, Czech Metrological Society, Czech National IMEKO Committee, Eurosensors Steering Committee, and the Advisory Board of SMM Conferences. From 2001 to 2005, he served as an Associated Editor of the IEEE SENSORS JOURNAL. He was a General Chairman of the Eurosensors XVI Conference held in Prague in 2002.

Michal Janošek was born in Varnsdorf, Czech Republic, in 1980. Graduated from the Faculty of Electrical Engineering, Department of Measurement – Measurement and Instrumentation, Czech Technical University, Prague in 2007. Currently working towards the Ph.D. degree at the same department.

His main research activity is the application of magnetic sensors in sensing and detection of ferromagnetic objects and further development in PCB fluxgate and AMR magnetometers and gradiometers. He is an author of six journal papers.